Insertion of Dipolar Molecules in Channels of a Centrosymmetric Organic Zeolite: Molecular Modeling and Experimental Investigations on Diffusion and Polarity Formation

Claire Gervais, Tino Hertzsch, and Jürg Hulliger*

Department of Chemistry and Biochemistry, University of Berne, Freiestrasse 3, CH-3012 Berne, Switzerland

Received: December 6, 2004; In Final Form: February 2, 2005

The mechanism of insertion of *p*-nitroaniline (PNA) and its diffusion behavior in channels of the hexagonal host structure of tris(*o*-phenylenedioxy)cyclotriphosphazene (TPP) was investigated by means of molecular modeling tools. Strong preferential sites in the bulk were found to be due to $\pi-\pi$ and NH$-\pi$ interactions between PNA and channel walls of TPP. MD simulations showed that diffusion can be characterized by jumps from one site to the next, occurring mainly because of the dynamic flexibility of the host structure. Calculations of host−guest interactions between the TPP surface and PNA approaching the entrance of channels with its terminal H_2N-first or O_2N-first revealed that the H_2N-first insertion is clearly preferred. Preferential insertion of PNA is found to be the reason for polar effects, observed experimentally. Because of a distinct guest−host recognition at the surface, guest−guest interactions were found to have a minor influence on polarity.

1. Introduction

The organic compound tris(*o*-phenylenedioxy)cyclotriphosphazene (TPP) is able to clarthrate a variety of small guest molecules by crystallizing into a hexagonal structure showing one-dimensional channels. The possibility to obtain guest-free hexagonal crystals and the reversibility of the adsorption−desorption process makes TPP to be one of the first organic structures recognized to feature zeolite-like properties. Originally studied by Allcock,[1] TPP became a compound of choice to investigate the structural features of organic zeolites and their potential applications. Studies focused on the stability of the hexagonal modification compared to compact guest-free monoclinic,[2] the investigation of gas storage or aromatic guest insertion by advanced NMR techniques,[3−5] the confinement of iodine molecules by several crystallization procedures,[6] and the insertion of dipolar molecules.[7]

In the later case, inclusion of long-prolate dipolar molecules of type A$-\pi-$D (with A and D being acceptor and donor groups, respectively) led to crystals showing pyroelectric and second-harmonic generation effects, confirming a mechanism of 180° orientational selectivity with respect to the different terminals of polar molecules. This phenomenon lies within the scope of a more general principle of polarity formation introduced first in 1999[8] which was extended thereafter to single component structures[9] and solid solutions.[10,11] This principle states that polarity can occur because the probabilities of docking on a growing *surface* dipolar molecules with A-first (↑) or D-first (↓) are different. In the case of host−guest systems,[12] this difference may be due to the loss of the center of symmetry (present in the bulk) at the surface and to selective interactions between guest molecules already entered into the channels and those arriving next.[7]

In the present paper, we investigate the insertion of *p*-nitroaniline (PNA) in TPP by using molecular modeling tools. This guest was chosen because of two interesting features: First, polar effects were observed, indicating an orientational selectivity of the TPP toward the insertion of PNA with H_2N-first or O_2N-first. Second, only a limited ratio of guests (no dense one-dimensional packing in channels) was found experimentally, suggesting the presence of preferential sites in the channels.

With the aim of understanding both aspects and because no detailed structural information could be obtained by X-ray diffraction, we performed the three following molecular modeling studies: (i) The potential energy surface of a PNA molecule entering the channel H_2N-first or O_2N-first was computed to understand *host−guest interactions* at the surface and within channels. (ii) PNA···PNA interactions taking place in TPP channels were calculated to probe the influence of *guest−guest interactions* on the packing of PNA. Finally, (iii) molecular dynamics simulations were performed to monitor *the mobility of the guests* in the TPP bulk. Two distinct aspects will be discussed, namely, the influence of the dynamic flexibility of the host structure on the stability of the system, including a measure for the balance between host−guest and guest−guest interactions in the formation of polarity.

2. Experimental Investigations

2.1. The TPP Structures. Tris(*o*-phenylenedioxy)cyclotriphosphazene (TPP) crystallizes in two different crystal structures. The compact monoclinic packing ($P2_1/n$; a = 25.086(5) Å, b = 5.911(2) Å, c = 25.913(7) Å, β = 95.97(2)°, calculated density = 1.596)[2] is composed of two molecules in the asymmetric unit. Both independent molecules are asymmetric (C_1), one being highly distorted and the other slightly deviating from symmetry D_{3h}.

In the presence of a suitable guest, a hexagonal structure is observed. Here, TPP molecules show a D_{3h} symmetry in accordance with the 3-fold symmetry of the packing, leading to $Z' = {}^1/_3$. The structure shows one-dimensional channels with a van der Waals diameter of ≈5 Å (Figure 1). The general hexagonal architecture is similar regardless of the inserted guest molecule. Only a small expansion or contraction of the lattice,

* To whom correspondence should be addressed. E-mail: juerg.hulliger@iac.unibe.ch.

10.1021/jp044464l CCC: $30.25 © 2005 American Chemical Society
Published on Web 03/24/2005

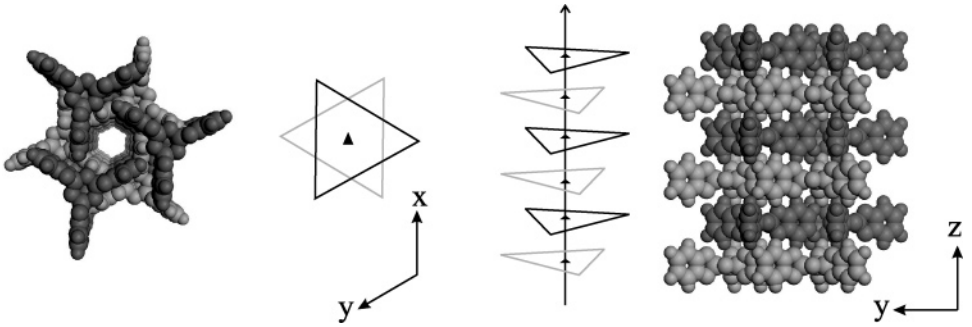

Figure 1. One-dimensional channels of the TPP hexagonal structure are composed of aromatic rings separated by *c*/2 (left). Two consecutive rings (light and dark gray) are rotated by 60° (right).

particularly in the (*x*, *y*) plane, was observed for accommodating guest molecules of different size. For instance, insertion of benzene leads to a host structure in space group $P6_3/m$ with $a = b = 11.804$ Å, $c = 10.054$ Å and calculated density = 1.257,[13] while insertion of water molecules gives $P6_3/m$, $a = b = 11.606(4)$ Å, $c = 10.087(3)$ Å and calculated density = 1.398.[2]

In contact with the liquid or the vapor of some guest compounds, monoclinic crystals of TPP can undergo a spontaneous transformation into the hexagonal form showing inclusion of guests into channels. Heating up crystals in a vacuum leads generally the conversion into the guest-free monoclinic form. However, the attribution of the term zeolite to TPP is justified by the possibility to obtain a guest-free channel structure with hexagonal symmetry by evacuation of volatile guests[3] particularly by reducing the crystal size.[14] Recently, Sozzani et al. succeeded in characterizing the guest-free hexagonal structure by single-crystal X-ray diffraction.[4]

2.2. The TPP−PNA System. Crystals of micrometer size (≈30−50 μm) of the hexagonal guest-free TPP structure were obtained by evaporation of THF (template) during 2 days at room temperature.[14] Such crystallites were then placed at 50 °C in an atmosphere saturated by *p*-nitroaniline. After several days, $TPP(PNA)_{0.5}$ was formed (stoichiometry determined by ^{1}H NMR; presence of the hexagonal lattice confirmed by X-ray powder diffraction data). Neither a longer in-diffusion time nor a higher temperature allowed an increase in the amount of PNA. Thermogravimetric measurements did not reveal a mass loss below 180 °C. The high temperature needed for removing the guests and a constant composition $TPP(PNA)_{0.5}$ are two arguments in favor of the presence of well-defined preferential sites exhibiting strong host−guest interactions.

Polar properties of $TPP(PNA)_{0.5}$ crystals were investigated by means of second-harmonic polarizing microscopy (SHM) and scanning pyroelectric microscopy (SPEM).[15] SHM has demonstrated a maximum response along the channel axis, showing no effect perpendicular to it. SPEM has revealed two opposite signs for the polarization with respect to both end faces of needle-shaped crystals. Both findings support a mechanism of a selectivity for PNA molecules entering H_2N-first or O_2N-first.

3. Molecular Modeling Studies

3.1. Validation of Force Field Parameters. Computational studies described in this paper were performed by using the module Discover of the software package Materials Studio[16] and the compass force field parametrized for phosphazenes.[17] Validation of the force field was checked by optimizing the monoclinic packing and the empty TPP host structure. The latter one was derived from the TPP−benzene experimental structure.[13] This choice was motivated by the volume and C-frame similarity between benzene and PNA. Full optimization (i.e., unit-cell parameters as well as intermolecular and intramolecular interactions allowed to relax) was performed by using the compass force field, with Ewald summation for both Coulombic and van der Waals interactions. A Newton procedure was used for the minimization step. Comparison was made with experimental monoclinic and hexagonal TPP−benzene structures from refs 2 and 13, respectively.

TABLE 1: Unit-Cell Parameters and Total Lattice Energy for the Two TPP Structures Optimized by Use of the Compass Force Field[17,a]

	monoclinic $P2_1/n$	hexagonal $P6_3/m$
energy (kJ/mol)	−796	−775
a (Å)	24.79 (−1.18%)	11.23 (−4.86%)
b (Å)	5.66 (−4.31%)	
c (Å)	25.25 (−2.54%)	10.08 (−0.29%)
β (deg)	97.8 (+1.9%)	
calcd density	1.74 (+8.96%)	1.38 (+2.14%)

[a] Percentages of deviation of experimental values from refs 2 and 13 are given in parentheses. Note that calculations were performed at 0 K and experimental data were collected at 298 K.

In both optimized structures, unit-cell parameters agree well with experimental data (maximum deviation of 5%), even though a tendency to obtain a denser packing was observed (Table 1). This can be partially explained when considering that optimization of the structure was made at zero kelvin, while experimental data were collected at room temperature (298 K). Furthermore, in the hexagonal packing the *c* value remains unchanged, while the reduction of the $a = b$ parameter reflects a shrinking due to empty channels (note that the hexagonal structure was optimized without a guest while benzene molecules are included in the experimental structure). This is in agreement with a fit of experimental data and indicates that the compass force field is suitable for describing TPP. The monoclinic packing has a lattice energy which is by 21 kJ/mol lower than that of the guest-free host structure.

3.2. Host−Guest Interactions. In a supercell $2 \times 2 \times 6$ joined to a vacuum slab of 100 Å, interaction energies (E_{HG}) between TPP and a PNA molecule moving along *c* from the vacuum to the bulk of the host structure were calculated (Figure 2). PNA positions are given by the Cartesian coordinates z_{guest} of its center of mass. Its polar state is defined by *up* or *down* (molecular axis *z* parallel to the *c* axis, with NO_2 and NH_2 pointing toward the channel, respectively). The TPP host surface is set up by the mean plane of the first aromatic ring that PNA will pass when entering into the host structure ($z_{surface}$ being thus approximately at 58 Å).

The following procedure was applied independently for a molecule PNA in *up* and *down* orientational state: (i) PNA was

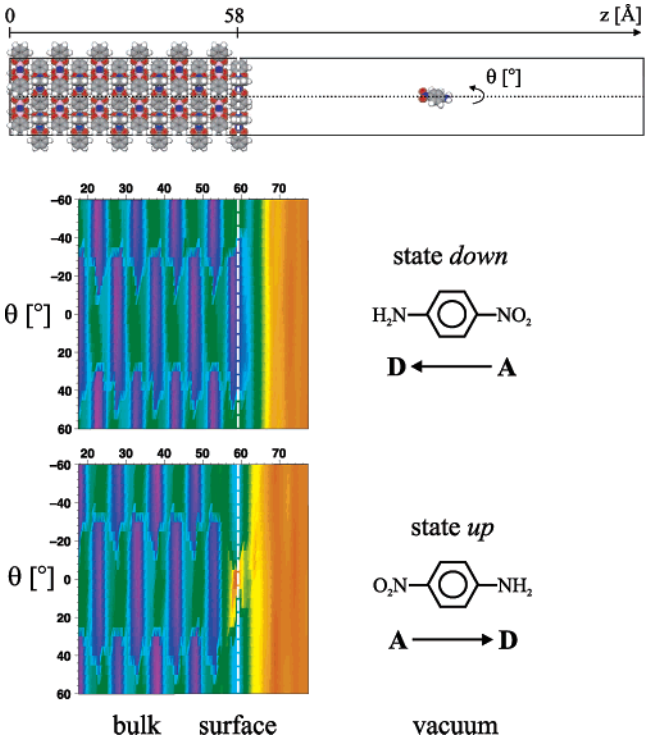

Figure 2. (upper) Periodic system used to compute host−guest interaction energies (E_{HG}). A molecule PNA is translated along z and rotated by θ with respect to the principal axis of the channel (dotted line). (lower) At each z and θ, energy minimization for PNA was performed (center of mass fixed) and E_{HG} was computed. Energy values can be identified by a color pattern varying from magenta ($E_{HG} \approx -40$ kJ/mol) to orange ($E_{HG} \approx 2$ kJ/mol). (Energy calculations were performed at 0 K.)

inserted in the supercell (care being taken to avoid sterical bumps) and the entire system was fully optimized. The guest was then moved along the c axis to place it in the vacuum slab. (ii) PNA was optimized with restraints applied on the center of mass (z_{guest} fixed) and E_{HG} was computed. This procedure was repeated for PNA rotated by $\theta = [-60°, -55°, ..., 60°]$ according to the principal axis of the channel. Step ii was repeated for PNA translated along the c axis by steps of 0.5 Å.

Interaction energies E_{HG} were calculated by using the compass force field. An atom-based summation with a cutoff distance of 30 Å (spline width, 10 Å; buffer width, 4 Å; van der Waals tail correction) was applied for both Coulombic and van der Waals interactions. Figure 2 (lower) shows the variation of E_{HG} with θ and z_{guest} for PNA either in state *up* or *down*. E_{HG} minima curves are plotted Figure 3.

Near the surface, PNA in state *down* makes interaction energies E_{HG}^{down} with TPP being about 10 kJ/mol lower than PNA in state *up* (E_{HG}^{up}). This energy difference, calculated at 0 K and by considering a planar and rigid TPP surface, is not indented to be exact. However, it gives an indication that *up* and *down* PNA molecules do not interact similarly with the surface: Although the TPP bulk structure is centrosymmetric and does not favor one of the two guest orientations, the surface (001), however, shows an *orientational selectivity* in favor of PNA in state *down*. The preference for molecules to enter H_2N-first can qualitatively be explained by the partially negatively charged surface of TPP, providing favorable interactions to the amino group ($\delta+$) but repulsive interactions with the partially negative NO_2 ($\delta-$) moiety.

In the bulk, deep energy minima ($E_{HG} \approx -40$ kJ/mol, depth of ≈15 kJ/mol) are observed. They are located every ≈5 Å but

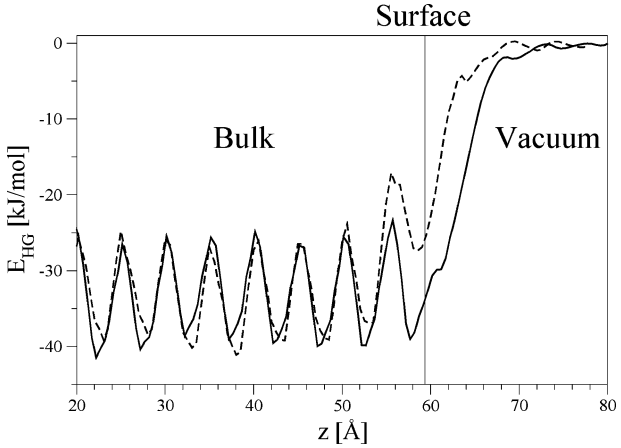

Figure 3. Host−guest interaction energies (E_{HG}) for inserting PNA in state *down* (full line, NH_2-first) and *up* (dashed line, NO_2-first). When the surface is approached (vertical line), the energy difference ($\Delta E_{HG} = E_{HG}^{up} - E_{HG}^{down}$) is about 10 kJ/mol. (Energy calculations were performed at 0 K.)

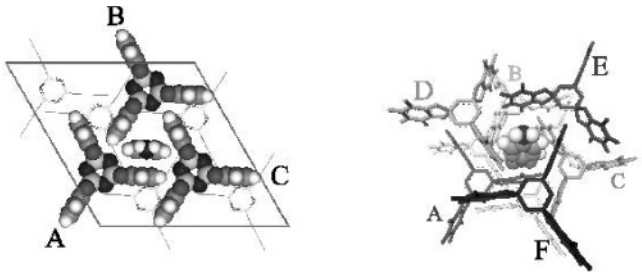

Figure 4. Position of PNA at a preferential site. The molecule optimizes the π stacking with TPP molecule A, as well as NH−π interactions with TPP molecules D, E and F. Energy values (calculated at 0 K) were found identical whatever the dipolar orientation of PNA was. Energies E_{HG}[kJ/mol] are −13.5 (A), −1.8 (B), −4.6 (C), −4.1 (D), −5.8 (E), −4.9 (F). A, B, and C represent $\pi-\pi$-stacking, D, E, and F are of the NH−π type.

rotated by $\theta \approx 60°$. A decomposition of E_{HG} between a PNA molecule situated in a preferential site and the neighboring TPP molecules could explain the deepness of these minima and their position along a channel (Figure 4): The phenyl core of PNA forms $\pi-\pi$ *stacking interactions*[18] with one of the three phenyl groups constituting the aromatic rings. As two consecutive rings are separated by $c/2$ and rotated by 60° according to the hexagonal packing, the same translational and rotational periodicity is found for PNA minima. Moreover, NH−π interactions[19] between the amino group and the aromatic channel walls are found to stabilize even more such preferential sites.

3.3. Guest−Guest Interactions. Guest−guest interaction energies (E_{GG}) were calculated by considering the previously described system in which a second PNA molecule was added for insertion: The first molecule PNA1 in state *up* or *down* was inserted into the bulk, being fully optimized. A second molecule PNA2 (state *up* or *down*) was then included into the channel and placed to stack above PNA1. These two molecules were optimized, and energies E_{GG} as well as E_{HG} were calculated (for optimization and energy calculation, see sections 3.1 and 3.2, respectively). Consistency of energy values was checked by following up this procedure using different initial PNA1−PNA2 distances (≈5 ± 1.5 Å, steps of 0.5 Å). Table 2 shows averaged energy values for the three types of contacts and minimum distances between the two nitrogen atoms involved in the interaction.

As might be expected, the acceptor−donor contact leads to the most favorable guest−guest interaction. Because E_{GG} values

TABLE 2: Bulk Guest−Guest and Host−Guest Interactions for Two PNA Molecules Inserted in the TPP Host Structure[a]

guest−guest contact	−A···D−	−D···D−	−A···A−
E_{GG} (kJ/mol)	−5.6	−2.6	+1.9
E_{HG} (kJ/mol)	−39.7	−37.5	−39.2
E_{total} (kJ/mol)	−85.0	−77.6	−76.5
distance N···N (Å)	4.27	3.22	6.88

[a] −A and −D states for $-NO_2$ and $-NH_2$ terminals, respectively. The total intermolecular energy (excluding host−host contacts) of the system is given by $E_{total} = 2E_{HG} + E_{GG}$. (Energy calculations performed at 0 K.)

are 1 magnitude lower than E_{HG} values, guest−guest interactions did not effectively influence the minimum host−guest interaction found for just one PNA ($E_{HG} \approx 40$ kJ/mol, only a small perturbation of E_{HG} appeared for the contact −D···D−). Therefore, localization of PNA molecules in channels of TPP is mainly driven by π interactions they exhibit by the channel wall. Contacts they could form with neighboring guests are not driving enough.

3.4. Molecular Dynamics Simulations. To study the influence of temperature and the dynamic flexibility of the host structure on the packing and diffusion properties of the guests, molecular dynamics (MD) simulations were performed. In a supercell 3 × 3 × 6 composed of four independent channels, PNA molecules (*all dipolar moments being parallel* within one channel) were inserted; care was taken to avoid sterical interference with each other and with the channel wall. Three bulk ratios TPP:PNA of 3:1, 2:1, and 1:1 were investigated by inserting one, four, and six molecules in each channel, respectively (see Figure 5, left side).

The three systems were fully minimized by using the force field procedure described in section 3.1. MD simulations were performed for a canonical ensemble (NVT) at three temperatures (300, 350, and 400 K). Temperatures were maintained constant by using a Berendsen thermostat[20] with a decay constant $\sigma = 0.10$. Periodic boundary conditions were applied. All the bonds were restrained to their current bond length up to a tolerance of 10^{-5} Å. The TPP host lattice was kept flexible. The Verlet algorithm[21] was used for integrating equations of motion, and time step was fixed to 0.5 fs. The total time of a MD simulation was typically of 200 ps (CPU time: 4−5 s per step, on current PCs).

At least 70 ps was required to equilibrate the system, i.e., for obtaining a stable total energy and pressure. This relatively long equilibration time can be explained by looking at mean square displacements (MSD) of TPP molecules (Figure 6).

For a crystal structure stable at the temperature of investigation, TPP molecules should remain in the solid state, with constant MSD.[21] The increase of MSD values with time is typical of molecules in the liquid state. In our case this is indicative for a degradation of the TPP lattice ending in a collapse of channels. At host−guest ratios of 3:1 and 2:1, the system turned out to be not stable for temperatures higher than 300 and 350 K, respectively. Only full loading (1:1) promoted a stable system whatever the temperature for investigating the time dependence was. These results are in agreement with experimental data showing that the guest-free hexagonal structure is metastable and converts generally spontaneously into the monoclinic form at temperatures above 320 K. Unfortunately, the small size of the supercell (limited to keep the computation time within reasonable limits; about 1 month per simulation) gave rise to some size effect (channels at supercell boundaries are empty) thus preventing further quantitative comparison between the stability of the systems studied by MD simulation and experimental data.

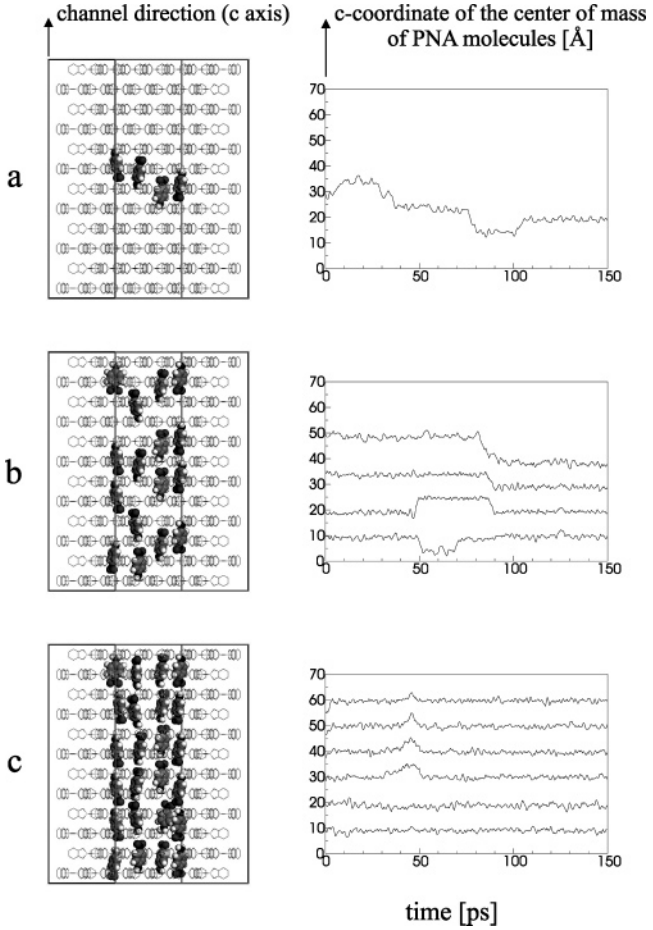

Figure 5. (left) Supercells 3 × 3 × 6 used for MD simulations and bulk ratios TPP:PNA of (a) 3:1, (b) 2:1, and (c) 1:1, corresponding to one, four, and six molecules per channel, respectively. (right) Typical trajectories at 300 K of PNA molecules for a single channel, showing the variation of z_{guest} of PNA molecules with respect to MD simulation time. Diffusion of guests is characterized by jumps of ≈5 Å, from one preferential site to the next one (steps seen in curves). Because of the need for cooperative jumps when loading increases, almost no diffusion is observed in case c.

Figure 5 (right) shows typical trajectories found for the three loadings applied. The diffusion of guest molecules can be characterized by jumps of ≈5 Å, corresponding to migrations of PNAs from one E_{HG} minimum to the next one. At intermediate loading (2:1), PNA molecules situated in neighboring preferential sites jump at the same time and in the same direction, indicating a *cooperative* diffusion process. At full loading (1:1), almost no diffusion was observed. MD simulations performed in the range of 300−400 K (steps every 25 K) for a system with fixed host structure showed no diffusion of PNA molecules below 375 K. The flexibility of TPP molecules is thus a necessary condition for lowering the barrier of activation, allowing PNA molecules to jump from one preferential site to the next one.

4. Discussion

4.1. Flexibility and Stability of the System. The weakness of van der Waals interactions holding the apohost together is found responsible for the low stability of the TPP structure compared to inorganic zeolites.[22−25] Such a fragile system can gain significant stabilization by host−guest contacts either

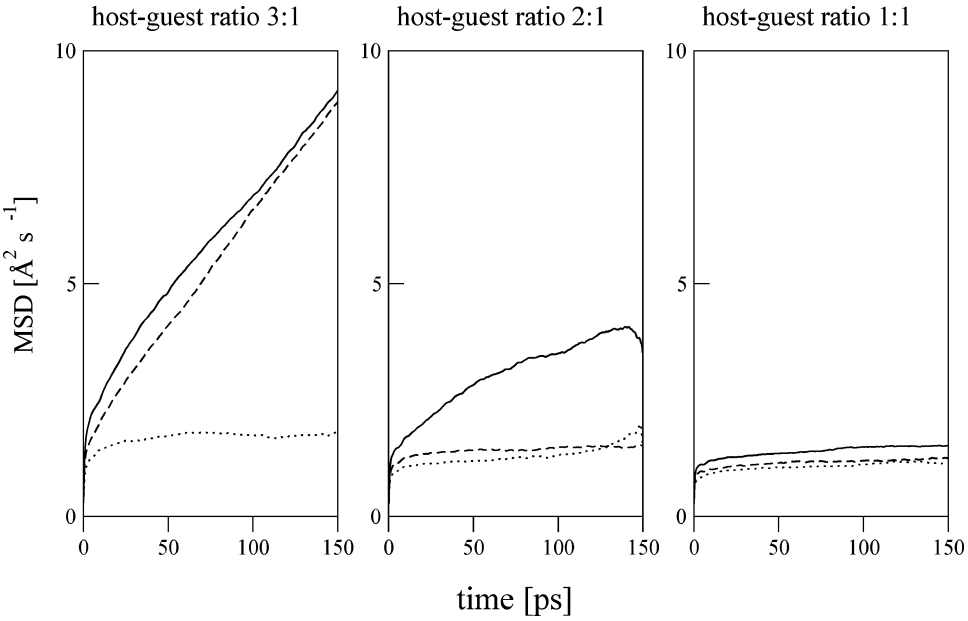

Figure 6. Mean square displacements (MSD) for TPP molecules given for three loadings at 300 K (dotted lines), 350 K (dashed lines), and 400 K (full lines).

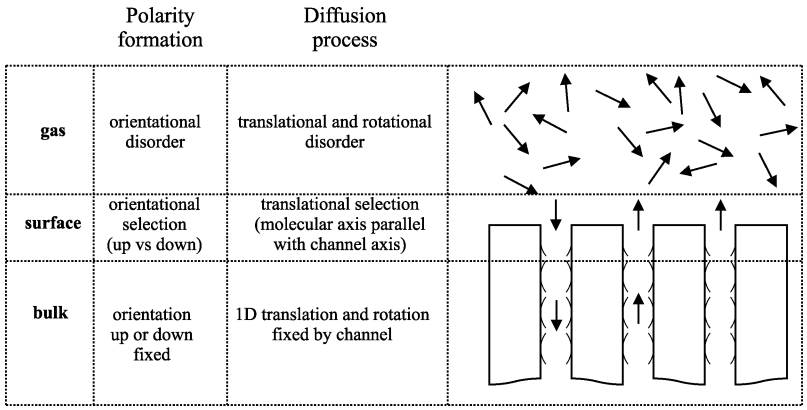

Figure 7. During the in-diffusion process, polarity formation can be explained by an equilibrium distribution of *up* and *down* molecules at the surface, which is equal to the ratio *up*/*down* found in the bulk. It is assumed that thermal relaxation has time to take place at the surface.

through close packing in one-dimension or by a less dense packing but with interactions being sufficiently strong (E_{HG}). In our case, the hexagonal structure is by 21 kJ/mol less stable than the monoclinic structure, requiring thus at least the same amount of host−guest interactions to compensate for. For the ratio found experimentally we have TPP(PNA)$_{0.5}$ (nE_{HG} = 0.5 × 40 kJ/mol = 20 kJ/mol). A rather simple calculation may thus allow a rough estimate for a minimum amount of guests needed for stabilizing the TPP host.

Another feature of van der Waals host structures is the high flexibility of molecules in these lattices. Dynamic flexibility seems to be essential[26] for the diffusion process of guests, which would remain trapped in their preferential sites in the case of a rigid host. Moreover, the slow diffusion observed for high ratios (i.e., (2:1) and (1:1), in which almost no diffusion was observed) can be explained not only by a need for cooperative jumps but also because a high amount of guests limits the flexibility of channels (Figure 6).

Therefore, a subtle balance seems to arise in TPP where strong host−guest interactions stabilize the system but consequently allow only for a slow diffusion process. For comparison, insertion of dipolar guest molecules in, e.g., perhydrotriphenylene,[27] a host structure exhibiting no functionalized channels, may give much weaker host−guest interactions and thus high diffusion efficiency or close packing along channels, as found experimentally for many types of guest molecules.

4.2. Polarity Formation. Two reasons are proposed for polarity formation: The first is arising from a difference of the interaction energy between the TPP surface and a PNA molecule entering a channel O_2N- or H_2N-first. The latter is favored when approaching the channel entrance, so that it is likely to be the preferential state for insertion of PNA. However, the influence of host−guest interactions can be concurrenced by guest−guest contacts. Even though 1 magnitude lower in energy, interactions between a molecule previously inserted and a guest approaching the channel entrance could play a non-negligible role for polarity formation.

Influence of host−guest and guest−guest interactions on polarity formation can be quantified by assuming that molecules approaching the channels have time to equilibrate their polar orientation and that their molecular axis is restricted to be parallel with the channel axis (Figure 7). In that case, host−guest energy difference at the surface is equivalent to calculated E_{HG} (Figure 2) and guest−guest interactions are given by E_{GG} values of Table 2. These energies are used to calculate the *equilibrium distribution* of molecules in state *up* and *down* at the surface. Any kind of kinetic effect giving rise to a deviation from the equilibrium distribution is not considered here. The

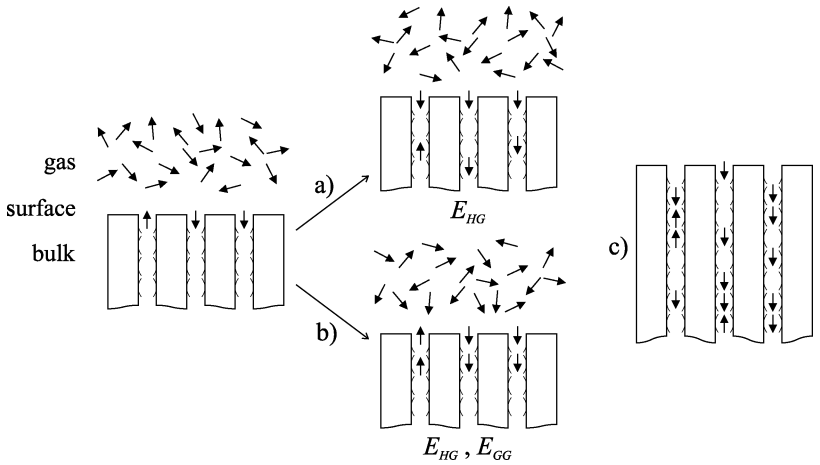

Figure 8. Process for entering guest molecules from the gas phase into channels. Once the first molecules are inserted, orientational selectivity of the molecules is driven either by (a) host−guest interactions or by (b) both host−guest and guest−guest interactions, according to the diffusion rate of guest molecules in TPP bulk. (c) Intermediate case of partial loading.

same ratio between *up* and *down* molecules is assumed to be found in the bulk. Polarity is thus expressed by $X_{net} = X_{down} - X_{up}$, where X_{down} and X_{up} are the molar fractions of molecules in state *down* and *up* at the surface, respectively.

In ref 12, a Markov process was proposed to calculate X_{net} in systems showing negligible host−guest interactions. In our case, in which both guest−guest and host−guest interactions are selective with respect to the state of PNA molecules at the surface, one has to consider the following in-diffusion process:

A first guest approaches the surface. Its probability of being in state *up* or *down* depends of the selectivity of the surface, i.e., of the difference of host−guest interaction energies ($\Delta E_{HG} = E_{HG}^{up} - E_{HG}^{down}$). Once the molecule is inserted, its state *up* or *down* cannot change with time (molecules cannot flip over in the bulk).

The inserted guest diffuses in the channel from the surface to the interior. This step is a prerequisite for in-diffusion of another guest.

A second guest enters the channel (Figure 8). Depending on the location of the guest already inserted (get close to surface or already deeply in), the orientational state of the entering molecule will be driven either by E_{HG} and E_{GG} or by E_{HG} only.

For the final amount of molecules included in state *up* and *down*, it is clear that diffusion of guests and the amount of loading become significant parameters for a calculation of X_{net} (Figure 8). Here, we restrict our calculations of X_{net} to the two limiting cases (for analytical treatment, see Appendix): (a) The approaching guest shows no interaction with an included guest molecule (X_{net} depends only on E_{HG}). (b) The approaching guest sees always a previously included molecule (X_{net} now depending on E_{HG} and E_{GG}). All intermediate situations give rise to X_{net} ranging between these two limiting cases. Figure 9 shows the variation of X_{net} for a host−guest energy difference $-10 < \Delta E_{HG} < 20$ kJ/mol, at temperatures 300 and 400 K. X_{net} values are clearly showing preferential insertion of molecules in state *down*, that is, with H_2N-first (Figure 9). In our case, where $\Delta E_{HG} \approx 10$ kJ/mol near the surface, the influence of guest−guest interactions is negligible ($X_{net} \approx 1$, for both cases (a) and (b)). Moreover, temperature does not have a strong impact on final result.

Therefore, final polarity in the TPP−PNA system is expected to be relatively stable toward both temperature variation and diffusion rate. This latter parameter can modify polarity in two different ways. At first, diffusion rate of molecules can be so high that thermal equilibrium cannot take place at the surface.

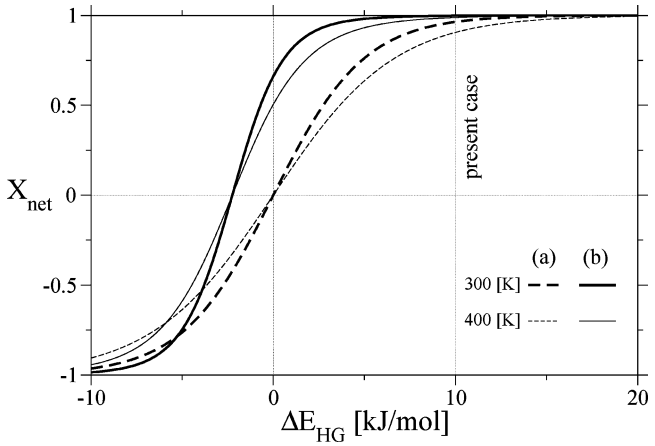

Figure 9. X_{net} as a function of ΔE_{HG}. Values were calculated at 300 and 400 K by either taking into account (a) only host−guest interactions or (b) both host−guest and guest−guest interactions. In the present system, $\Delta E_{HG} = E_{HG}^{up} - E_{HG}^{down}$ were found to be ≈10 kJ/mol near the surface (see Figure 3).

As said above, this effect is assumed to be neglected, because in-diffusion of PNA molecules from the gas to the bulk is relatively slow. Second, diffusion rate is responsible for the probability of the presence of guest−guest recognition at the surface. Calculations of X_{net} by taking the two limiting cases (a and b) showed that diffusion rate does not have a great influence on polarity formation.

In this respect, polarity formation in the TPP−PNA system is a phenomenon *independent of kinetic effects*. The model proposed here to calculate the equilibrium distribution between *up* and *down* states is similar to that used to depict polarity being formed during close-to-equilibrium growth of single-[28] and two-component crystals.[11] Comparable studies explaining surface-induced properties by using a model based on thermodynamic considerations and assuming *fast surface equilibration* can be found in the literature.[29,30]

5. Conclusion

Calculations of guest−guest and host−guest interactions in the bulk and at the surface, as well as MD simulations of the system at different temperatures and ratios of loading allowed the following indications about TPP−PNA:

In the bulk, PNA molecules are docked to preferential sites forming strong $\pi-\pi$ and NH$-\pi$ interactions with the channel

wall. Their diffusion, characterized by jumps from one site to another, is made possible by the flexibility of the TPP host structure which lowers the energy barrier for diffusion. A minimum amount of inserted PNA molecules is necessary to stabilize the TPP hexagonal structure. The minimum loading found by calculation is one guest per two host molecules, a ratio in agreement with experiments. In that case, the energy E_{HG} counterbalances the lattice energy difference separating the two structures of TPP.

The partially negative charge of the hexagonal TPP surface is made responsible for a selectivity of insertion into channels of PNA molecules with their terminal H_2N-first. The selectivity by the surface has been quantified by $\Delta E_{HG} \approx 10$ kJ/mol, which corresponds to the host−guest energy difference when entering a molecule in state *down* (H_2N-first) vs state *up* (O_2N-first). Polar effects (expressed by $X_{net} = X_{down} - X_{up}$) have been quantified for two limiting cases: The approaching molecule makes contacts only (a) with the host surface or (b) with both the surface and an already included guest. In both cases, almost all the in-diffused PNA molecules are in state *down*. The final state of the crystal is therefore expected to be bipolar in case of in-diffusion of molecules from both ends of a crystal (corresponding to faces {001} where the channel entrances are) or unipolar if diffusion is allowed from only one side of the crystal.[6]

From a general point of view,[8] it has been shown that a centrosymmetric host structure, i.e., its surface, shows recognition properties against a vectorial object, leading thus to observable polar properties as theoretically predicted. In the present example, it is shown that polarity is due to a difference of host−guest interactions between the TPP surface and the two terminals of the PNA vector, rather than to preferential guest−guest interactions between the approaching PNA and molecules already included. However, in the case E_{GG} would become predominant for orientational selectivity (which is not the case here), diffusion of the guests and loading of the channels should be both considered in the calculation because then they would influence the probability of occurrence of guest−guest contacts.

Acknowledgment. The authors thank Thomas Wüst for help in calculating X_{net} values and Professor Bürgi for fruitful discussions. The Swiss National Science Foundation (Project No. 200021-101658/1) is acknowledged for financial support.

Appendix

When a molecule approaches the surface, distinct situations summarized in Figure 10 may arise. For calculation, we consider that polarity is expressed by $X_{net} = X_{down} - X_{up}$, with X_{down} and X_{up} molar fractions of molecules in state *down* and *up*, respectively ($X_{down} + X_{up} = 1$).

Case a: If only host−guest interactions are present when a guest molecule approaches the surface, X_{net} is given by

$$X_{net} = \frac{1 - e^{-\Delta E_{HG}/RT}}{1 + e^{-\Delta E_{HG}/RT}} \tag{1}$$

with $\Delta E_{HG} = E_{HG}^{up} - E_{HG}^{down}$.

Case b: If a molecule makes host−guest as well as guest−guest contacts when approaching the surface, the process of polarity formation can be described as a Markov chain.[32,33] Transition probabilities P_{ij} related to the insertion of a molecule with its terminal i = A, D making interaction with the terminal

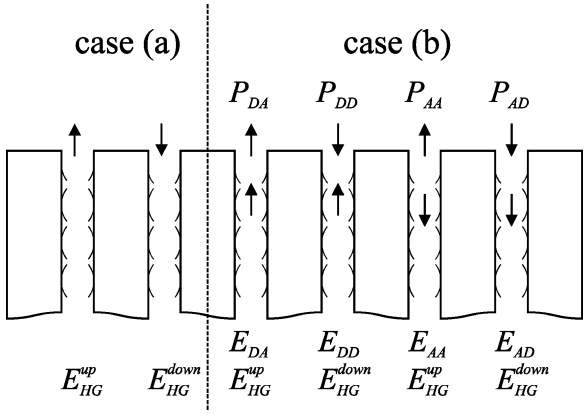

Figure 10. Guest−guest and host−guest interaction energies taking place in cases a and b. E_{ij} are guest−guest interaction energies between molecular terminals i = A, D of the already included guest and j = A, D of the approaching guest, where A and D correspond to acceptor and donor terminals, respectively. E_{HG}^{up} and E_{HG}^{down}: labeling host−guest interaction energies between the surface and a guest molecule in states *up* and *down*, respectively.

j = A, D of a guest already in the channel are defined as

$$P_{ij} = \frac{1}{1 + f_{ij}}, \qquad i, j = \text{A, D} \tag{2}$$

where X_{net} is given by

$$X_{net} = \frac{P_{DD} - P_{AA}}{P_{DD} + P_{AA}} \tag{3}$$

Corresponding functions f_{ij} are

$$f_{AD} = \exp\{(-\Delta E_A - \Delta E_{HG})/RT\} \tag{4}$$

$$f_{AA} = \exp\{(\Delta E_A + \Delta E_{HG})/RT\} \tag{5}$$

$$f_{DA} = \exp\{(-\Delta E_D + \Delta E_{HG})/RT\} \tag{6}$$

$$f_{DD} = \exp\{(\Delta E_D - \Delta E_{HG})/RT\} \tag{7}$$

with $\Delta E_A = E_{AA} - E_{AD}$, $\Delta E_D = E_{DD} - E_{DA}$.

This finally leads to

$$X_{net} = \frac{e^{(\Delta E_A + \Delta E_{HG})/RT} - e^{(\Delta E_D - \Delta E_{HG})/RT}}{2 + e^{(\Delta E_A + \Delta E_{HG})/RT} + e^{(\Delta E_D - \Delta E_{HG})/RT}} \tag{8}$$

Note that setting $\Delta E_{HG} = 0$ leads to an equation given in ref 34 (a Markov chain with guest−guest interactions only) or $\Delta E_A = \Delta E_D = 0$ leads to eq 1, which corresponds to case a (host−guest interactions only).

References and Notes

(1) Allcock, H. R.; Siegel, L. A. *J. Am. Chem. Soc.* **1964**, *86*, 5140−5144.
(2) Allcock, H. R.; Levin, M. L.; Whittle, R. R. *Inorg. Chem.* **1986**, *25*, 41−47.
(3) Sozzani, P.; Comotti, A.; Simonutti, R.; Meersmann, T.; Logan, J. W.; Pines, A. *Angew. Chem.* **2000**, *112*, 2807−2810.
(4) Sozzani, P.; Braco, S.; Commoti, A.; Ferretti, L. Simonutti, R. *Angew. Chem.*, in press.
(5) Sozzani, P.; Comotti, A.; Bracco, S.; Simonutti, R. *Angew. Chem., Int. Ed.* **2004**, *43*, 2792−2797.
(6) Hertzsch, T.; Budde, F.; Weber, E.; Hulliger, J. *Angew. Chem., Int. Ed.* **2002**, *41*, 2282−2284.
(7) Hertzsch, T.; Kluge, S.; Weber, E.; Budde, F.; Hulliger, J. *Adv. Mater.* **2001**, *13*, 1864−1867.
(8) Hulliger, J. *Z. Kristallogr.* **1999**, *214*, 9−13.

(9) Gervais, C.; Wüst, T.; Behrnd, N.-R.; Wübbenhorst, M.; Hulliger, J. *Chem. Mater.* **2005**, *17*, 85−94.

(10) Wüst, T.; Gervais, C.; Hulliger, J. *Cryst. Growth Des.* **2005**, *5*, 93−97.

(11) Wüst, T.; Hulliger, J. *J. Chem. Phys.* **2005**, *122*, 084715.

(12) Hulliger, J.; Rogin, P.; Quintel, A.; Rechsteiner, P.; König, O.; Wübbenhorst, M. *Adv. Mater.* **1997**, *9*, 677−680.

(13) Allcock, H. R.; Allen, R. W.; Bissell, E. C.; Smeltz, L. A.; Teeter, M. *J. Am. Chem. Soc.* **1976**, 5120−5125.

(14) Hertzsch, T.; Gervais, C.; Hulliger, J.; Jäckel, B.; Guentay, S.; Bruchersteifer, H.; Neels, A. Submitted to *Microporous Mesoporous Mater.* **2005**.

(15) Hulliger, J. *Chimia* **2001**, *55*, 554−561.

(16) Materials Studio by Accelrys Inc.

(17) Sun, H.; Ren, P.; Fried, J. R. *Comput. Theor. Polym. Sci.* **1998**, *8*, 229−246.

(18) Tsuzuki, S.; Honda, K.; Uchimaru, T.; Mikami, M.; Tanabe, K. *J. Am. Chem. Soc.* **2002**, *124*, 104−112.

(19) Tsuzuki, S.; Honda, K.; Uchimaru, T.; Mikami, M.; Tanabe, K. *J. Am. Chem. Soc.* **2000**, *122*, 11450−11458.

(20) Berendsen, H. J. C.; Postma, J. P. M.; van Gunsteren, W. F.; DiNola, A.; Haak, J. R. *J. Chem. Phys.* **1984**, *81*, 3684−3690.

(21) Allen, M. P.; Tildesley, D. *Molecular Simulation of Liquids*; Oxford University Press: Oxford, 1980.

(22) Raj, N.; Sastre, G.; Catlow, C. R. A. *J. Phys. Chem. B* **1999**, *103*, 11007−11015.

(23) Demontis, P.; Stara, G.; Suffritti, G. B. *J. Chem. Phys.* **2004**, *120*, 9233−9244.

(24) Li, J. Y.; Yu, J. H.; Xu, R. R. *Chin. J. Inorg. Chem.* **2004**, *20*, 1−16.

(25) Schuring, D.; Jansen, A. P. J.; van Santen, R. A. *J. Phys. Chem. B* **2000**, *104*, 941−948.

(26) Leroy, F.; Rousseau, B.; Fuchs, A. H. *Phys. Chem. Chem. Phys.* **2004**, *6*, 775−783.

(27) Hulliger, J.; König, O.; Hoss, R. *Adv. Mater.* **1995**, *7*, 719−721.

(28) Bebie, H.; Hulliger, J.; Eugster, S.; Alaga-Bogdanovic, M. *Phys. Rev. E: Stat. Phys., Plasmas, Fluids, Relat. Interdiscip. Top.* **2002**, *66*, 021605.

(29) Drossel, B.; Kardar, M. *Phys. Rev. E: Stat. Phys., Plasmas, Fluids, Relat. Interdiscip. Top.* **1997**, *55*, 5026−5032.

(30) Froyen, S.; Zunger, A. *Phys. Rev. Lett.* **1991**, *66*, 2132−2135.

(31) Hulliger, J.; Roth, S. W.; Quintel, H.; Bebie, H. *J. Solid State Chem.* **2000**, *152*, 49−56.

(32) Harris, K. D. M.; Jupp, P. E. *Chem. Phys. Lett.* **1997**, *274*, 525−534.

(33) Harris, K. D. M.; Jupp, P. E. *Proc. R. Soc. London, Ser. A* **1997**, *453*, 333−352.

(34) Hulliger, J. In *Encyclopedia of Supramolecular Chemistry*; Marcel Dekker: New York, 2004; pp 1120−1128.